5.1. Introduction

High dielectric constant materials have attracted attention due to their application as energy storage materials which play a vital role in stable power systems, hybrid electric vehicles, mobile electronic and pulsed power devices [Nalwa *et al*. (1999), Saka & Datta *et al*. 2001].There are two major types of ceramic materials traditional and advanced over the traditional ones include clay products, silicate glass, and cement. While advanced ceramics consist of pure oxides (Al_2O_3), carbides (SiC), nitrides (Si_3N_4), perovskite (ABO_3), non-silicate glasses and many others [Yadav & Gautam *et al*. (2014), Rödel *et al*. (2009)]. ABO_3 type oxide materials exhibit the physical properties of industrial importance such as electrical, dielectric, ferroelectricity, anti-ferroelectricity, and piezoelectricity, as well as insulating, semiconducting, metallic and ferromagnetic behaviours. More recently, researchers have also begun to actively include sensing, actuation, computation and communication into composites [McEvoy & Correll *et al*. (2015)]. The interesting feature is that all these giant dielectric constant materials have similar dielectric behaviour to CCTO, i.e., they all exhibit a Debye-like relaxation and their dielectric constants are nearly independent of frequency and temperature well below the relaxation frequency [Singh *et al*. (2015)]. Most of the current studies on dielectric polymer composites focus on the enhancement of the dielectric permittivity using ferroelectric metal oxides Pb(Zr, Ti)O_3 (PZT), Pb($Mg_{0.33}Nb_{0.77}$)O_3 - PbTiO$_3$ (PMNT), and BaTiO$_3$ (BTO). BaTiO$_3$ is known to be relaxor ferroelectrics such as Pb($Mg_{1/3}Nb_{2/3}$)O_3 [PMN], Pb($Zn_{1/3}Nb_{2/3}$)O_3 [PZN] and Pb$_{1-x}$La$_x$(Zr$_{1-y}$Ti$_y$)O_3 [PLZT] [Moulson & Herbert *et al*. 2003]. The Pb-based perovskite oxides are not environmental friendly capacitor materials, Ferroelectric perovskite BaTiO$_3$ shows phase transitions exhibits high dielectric constant ($\varepsilon_r \sim$ 1000-20000). Recently studied on ACu$_3$Ti$_4$O$_{12}$ (A = Ca, La, Gd, Sm, Dy, Y and Bi) oxide materials with a complex perovskite structure, having general formula

$CaCu_3Ti_4O_{12}$, $Bi_{2/3}Cu_3Ti_4O_{12}$, $La_{2/3}Cu_3Ti_4O_{12}$, and $Y_{2/3}Cu_3Ti_4O_{12}$, attracted the attention of technologists and scientists due to their high dielectric constant [Singh et al. (2014), Subramanian *et al*. (2000)]. $Bi_{2/3}Cu_3Ti_4O_{12}$ (BCTO) is one of the members of the family $ACu_3Ti_4O_{12}$ which is isostructurally similar to $CaCu_3Ti_4O_{12}$ (CCTO). However, limited research literature report was available on BCTO ceramics [Szwagierczak *et al*. (2008), Hao *et al*. (2009), Liu *et al*. (2004)]. Recently CCTO based many composite materials have been studied to improve the dielectric properties using Al_2O_3 [Warangkanagoo & Rujijanagul *et al*. (2012)], TeO_2 [Amaral *et al*. (2011)], GeO_2 [Amaral *et al*. (2010)], Cr_2O_3 [Kwon *et al*. (2008)], SiO_2 [Kim *et al*. (2007)], ZnO [Chen *et al*. (2013)], $CaTiO_3$ [Fang *et al*. (2006)], $SrTiO_3$ [Yan *et al*. (2006)] and $Ba_{0.6}Sr_{0.4}TiO_3$ [Yu *et al*. (2008)], The increase of grain boundary resistance or barrier layer due to those oxides result in lower dielectric losses due to the internal barrier layer capacitance.

In the present study, the nano-sized composite of $0.5BaTiO_3$ - $0.5Bi_{2/3}Cu_3Ti_4O_{12}$ (BT-BCT 5) were synthesized by a solid-state method to improve the dielectric properties. This technique has advantages including low processing costs, energy efficiency, and high production rate. The nanocomposite ceramic BT-BCT 5 was synthesized by the solid state method have been characterized by XRD, SEM, TEM, AFM and dielectric properties were also evaluated to understand the best features developed in this composite.

5.2. Experimental

5.2.1. Synthesis

The nanocomposite ceramic of $0.5BaTiO_3$-$0.5Bi_{2/3}Cu_3Ti_4O_{12}$ (BT-BCT 5) was manufactured by a modified solid-state route via three steps. Firstly $Bi_{2/3}Cu_3Ti_4O_{12}$ (BCTO) was synthesized by the citric nitrate gel route using analytical grade

$Bi(NO_3)_2.4H_2O$ (99.5% Qualigens, India), $Cu(NO_3)_2.3H_2O$ (99.5% Merck, India), Solid TiO_2 (99.5% Merck, India), as the starting materials. In this route, their stoichiometric amounts were mixed in a beaker along with solid TiO_2. Secondly, $BaTiO_3$ (BTO) was prepared by semi wet sol-gel process using $Ba(NO_3)_2.TiO_2$ (99.5% Merck, India), and citric acid (99.5% Merck, India) as the starting materials. In this route their stoichiometric amounts were mixed in a beaker along with solid TiO_2, then citric acid (equivalent to metal ions) was added to the solution. The consequential solution was heated on a hot plate under stirring at 70 - 80 $^\circ$C to evaporate the water and allow self-ignition. At room temperature, ignition process was carried out in air, which exhausted a lot of gasses and formed a fluffy mass of BTO and BCTO ceramic powders. In this process the mixing of a solution of a metal precursor and a polyfunctional organic acid having at least one hydroxyl group and one carboxylic acid group such as citric, glycine, tartaric or glycerol. Citric acid as a complexion agent can form a complex with cations at both the carboxylic end and provide the fuel for the ignition step. The gel of BTO and BCTO were calcined in air at 800 °C for 6 h in an electrical furnace. A thirdly amount of the prepared powders of BTO and BCTO by a semi-wet sol-gel process was mixed. In this process, we used calcined powder of BTO and BCTO as raw materials to synthesize the BT-BCT 5 nanocomposite ceramic to develop the new modified solid state route to get a nanometer range particles with foreseen properties. The mixed BT-BCT 5 nanocomposite ceramic particles with to 2 wt. % polyvinyl alcohol (PVA) were pressed into cylindrical pellets using a hydraulic press. The PVA binder was burnt out at 500 °C for 5 h. Finally, the BT-BCT 5 nanocomposite pellets were sintered at 870 °C for 4 h, 8 h, 12 h and 16 h.

5.2.2. Characterization

The crystalline phases of BT-BCT 5 nanocomposite sintered samples were identified by using the X-ray diffraction analysis (Rigaku, miniflex-600, Japan) employing Cu-kα radiation. The microstructures of the fractured surface of sintered ceramics were examined using a scanning electron microscope (Ziess EVO-18) and the particle size was observed using a high-resolution transmission electron microscope (Tecnai G^2 20 TWIN). For transmission electron microscopy (TEM) observation, the powder sample of BTBCT 5 nanocomposite was used for ultrasonication in acetone medium and then the suspended powders were dispersed in the carbon coated copper grid followed by drying in hot air oven. This copper coated grid containing the powder sample was used in the electron microscope. The surface morphology was analysed by atomic force microscopy [AFM Nano Drive Dimension Edge 8.06 (Build R1MN. 1199088)]. The specimens were prepared by dispersing the sintered BT-BCT 5 nanocomposite powder in acetone by Ultrasonication, and this type of suspensions was deposited onto the glass slides. The BT-BCT 5 nanocomposite sintered pellets were polished using SiC abrasive paper until they had a surface like a mirror finish. Silver paste was applied to both sides of the round faces of the ceramic pellets for the purpose of the dielectric and electrical measurements. The dielectric and electrical data of the BT-BCT 5 nanocomposite ceramic was obtained using an LCR meter (PSM 1735, NumetriQ 4th Ltd, and U.K.) over the frequency range of 100 Hz – 5 MHz and in the temperature range of 300 – 500 K.

5.3. Results and Discussion

5.3.1. X-ray diffraction studies

Figure 5.1 Shows the XRD pattern of the BT-BCT 5 nanocomposite ceramic sintered at 870 °C for 4 h, 8 h and 12 h and 16 h. The XRD pattern of the ceramic shows the presence of both phases of $BaTiO_3$ (JCPDS – 89-2475), and $Bi_{2/3}Cu_3Ti_4O_{12}$ (JCPDS – 80-1343) in the ceramic sample sintered for different sintering durations. XRD also shows the presence of split peaks for reflections (2 2 0), (2 11) and (4 0 0) due to the presence of Cu $K\alpha_2$ along with Cu-$K\alpha_1$ in the X-ray radiation used for diffraction. XRD data was also used to determine the average crystallite size (D) of the BT-BCT 5 nanocomposite ceramics at different sintering duration using a line broadening method. The Cauchy component of the Voigt function represents the crystallite size, in the single line analysis method, the crystallite size (D) of the BT-BCT 5 nanocomposite at different sintering duration was estimated using the equation 2.2. Further to get correct values for crystallite size, line broadening due to instrumental effect (β_i) was removed by using the XRD data for the standard sample. The average crystallite sizes derived from the five XRD data were 24 nm, 26 nm, 56 nm and 43 nm for the BT-BCT 5 nanocomposite ceramic sintered for 4 h, 8 h, 12 h and 16 h respectively.

Density can indicate a change in the composition of a material, or a defect in a product, such as a crack or a bubble in cast parts (known as voids), for instance in sanitary ceramics. Density measurement of sintered BT-BCT 5 sample was recorded employing Archimedes Principle. The density of BT-BCT 5 is found to be 6.033 gcm^{-3}.
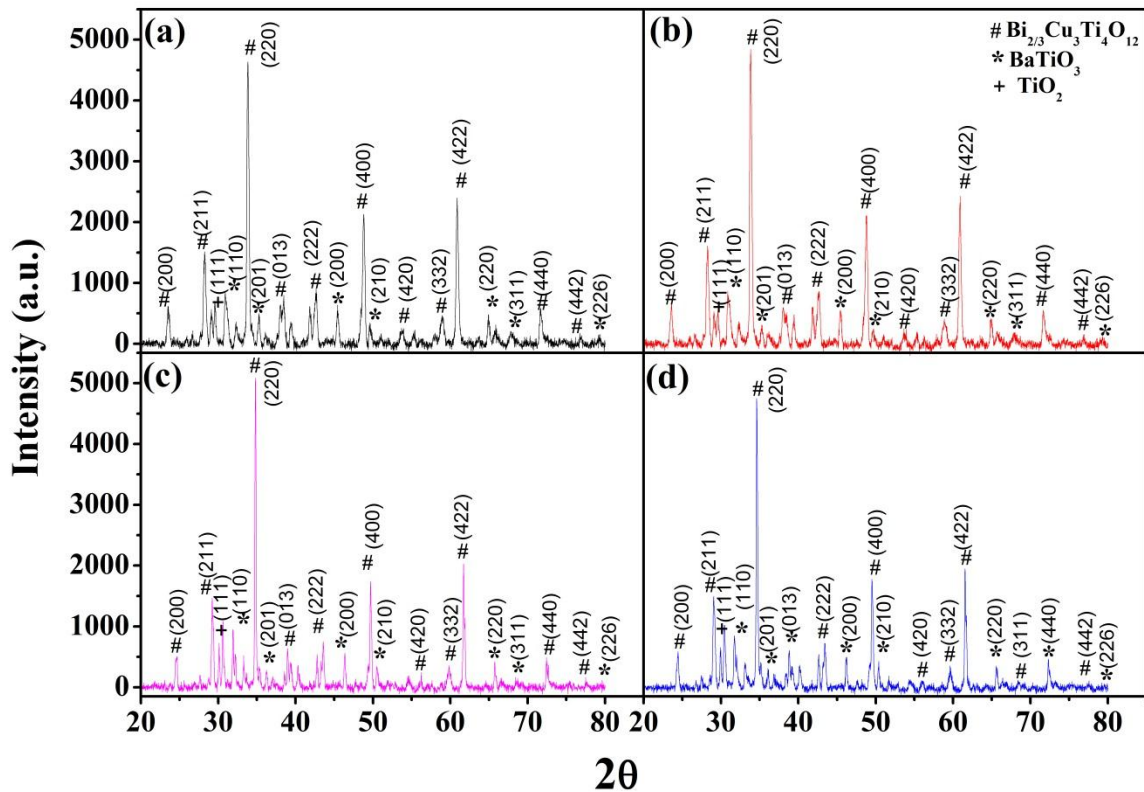
Figure 5.1. X-ray powder diffraction patterns of BT-BCT 5 nanocomposite sintered at 870 °C for (a) 4 h   (b) 8 h (c) 12 h and (d) 16 h.

### 5.3.2. Microstructural studies

Figure 5.2(a) shows the bright field TEM image of the BT-BCT 5 nanocomposite ceramic sintered at 870 °C for 12 h. The image of nanocomposite ceramic demonstrates the presence of nanocomposite in size range of 90 ± 10 nm. It is also revealed that the ceramic powder was found to be nanocrystalline in nature. It is also seen that the particles sizes observed by TEM are not in agreement with the average crystallite size determined

by XRD. These differences could be attributed to the formation of particles with the combination of low crystallites.
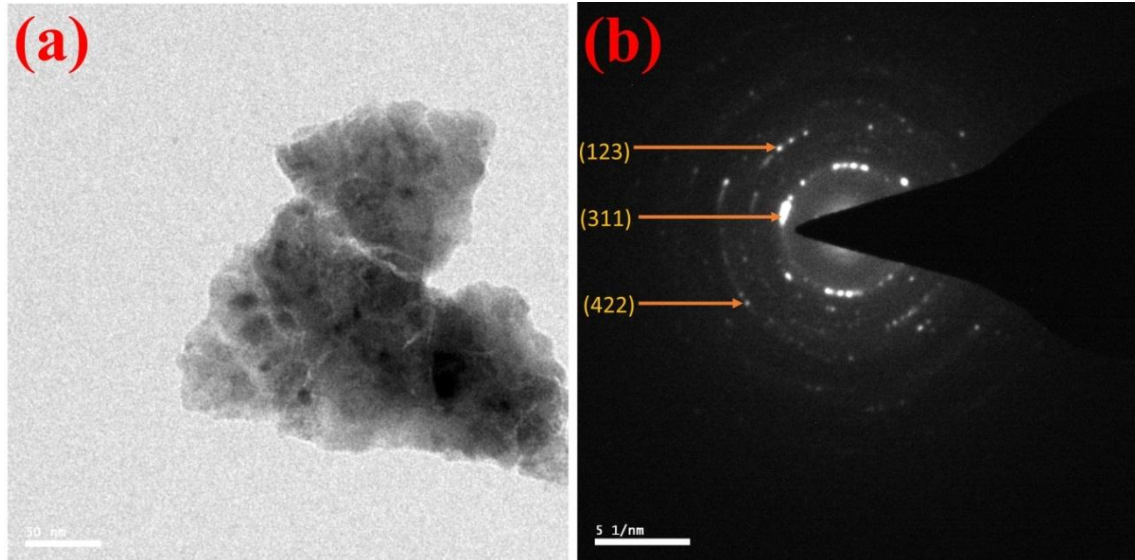
Figure 5.2. (a) Bright field TEM images and (b) SEAD pattern of BT-BCT 5 nanocomposite sintered at 870 °C for 12 h.

Figure 5.2(b) shows the selected area electron diffraction patterns (SADP) of BT-BCT 5 nanocomposite ceramic which confirmed the polycrystalline nature of material. The interplaying d-spacing (h k l) measured from the SAED are in good agreement with the values obtained from XRD data [Yadava *et al*. (2016)]. The additional spots observed in the SADP patterns were from the adjacent grains and subgrains because of their orientation in a different direction.
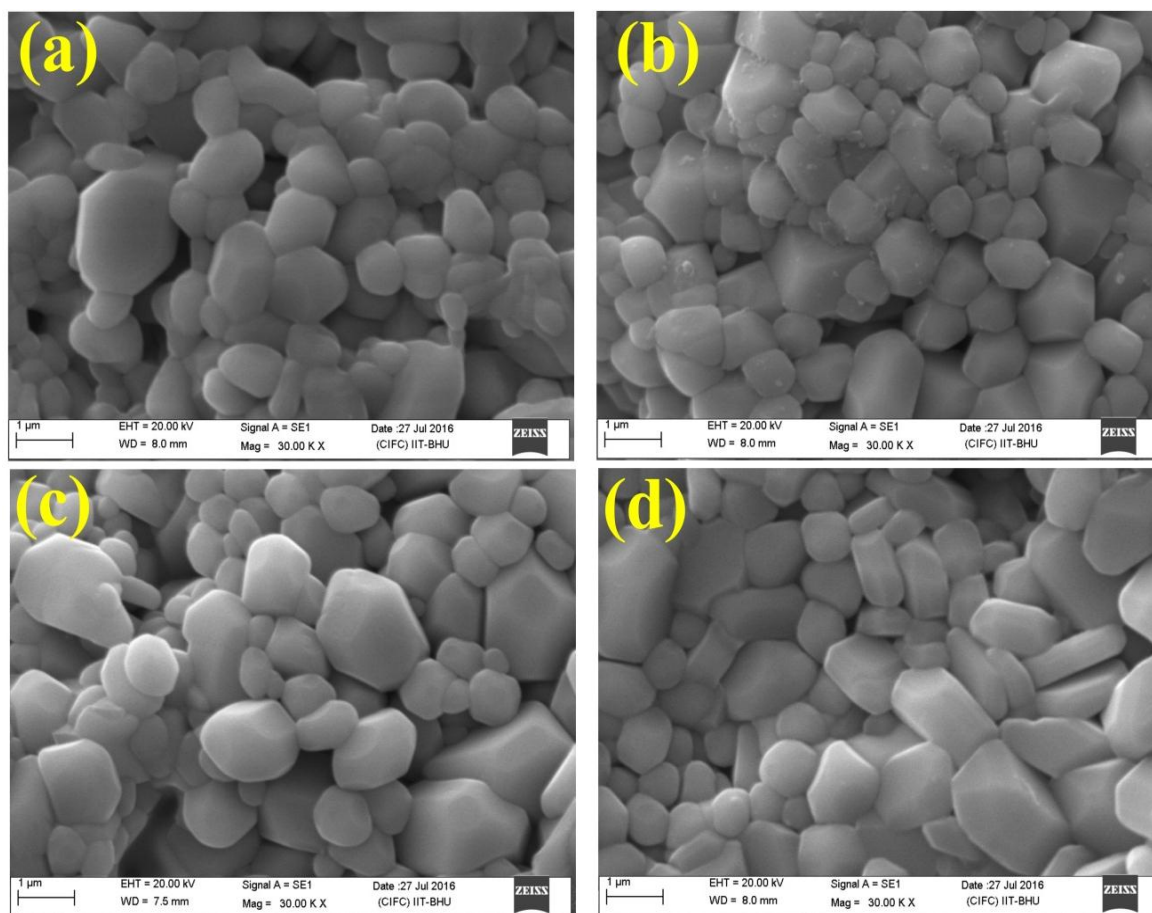
Figure 5.3. SEM micrographs of BT-BCT 5 nanocomposite sintered at 870 °C for (a) 4 h (b) 8 h (c) 12 h   and (d) 16 h.

Figure 5.3 shows microstructure of the surface morphology obtained by SEM of the BT-BCT 5 nanocomposite ceramics sintered at 870 °C for 4 h, 8 h, 12 h and 16 h. It is clearly seen that microstructure of BT-BCT 5 nanocomposite with the increase in sintering duration image showed packed faceted grain morphology with varying grain size in the range of 1.0 - 2.5 μm. It is also observed that the grain size increases with increasing sintering duration. The AFM images are shown in Figure 5.4(a) and (b) of the BT-BCT 5 nanocomposite powder sintered at 870 °C for 12 h which indicates that the bimodal nature of BT-BCT 5 nanocomposite. The average roughness and root mean square (RMS) data were obtained as 4.3 nm and 13.0 nm respectively on scanned area 20

μm × 20 μm where ten different points were used for the calculation of mean value [Khare *et al*. (2016)]. Figure 5.4(c) shows the histogram of particle roughness and Figure 5.4(d) demonstrates the histogram of particle sizes of BT-BCT 5 nanocomposite ceramic recorded by AFM using tapping mode. It is observed from the figure that the most of the particles are in a range of 100 nm to 250 nm. The average size and area of particles were found to be 0.3 μm and 400 μm^2 respectively which are also substantiated by SEM analysis.
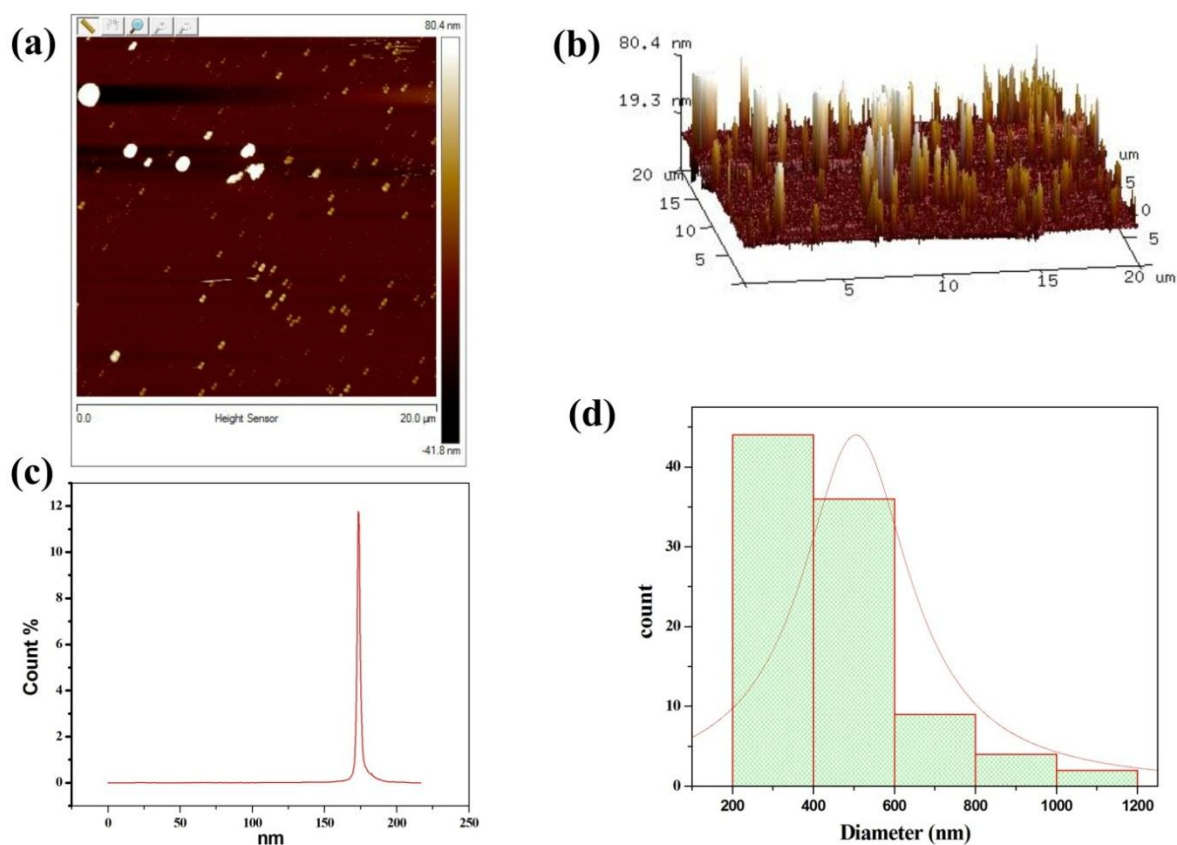
Figure 5.4. AFM images of BT-BCT 5 nanocomposite sintered at 870 °C for 12 h (a) 2 dimensional (b) 3D structure (c) depth histogram (d) bar diagram of particles size.

5.3.3. Dielectric studies

The variations in dielectric constant with temperature for the BT-BCT 5 nanocomposite sintered at 870 °C for 4, 8, 12 and 16 h at few selected frequencies is shown in **Figure** 5.5(a-d).
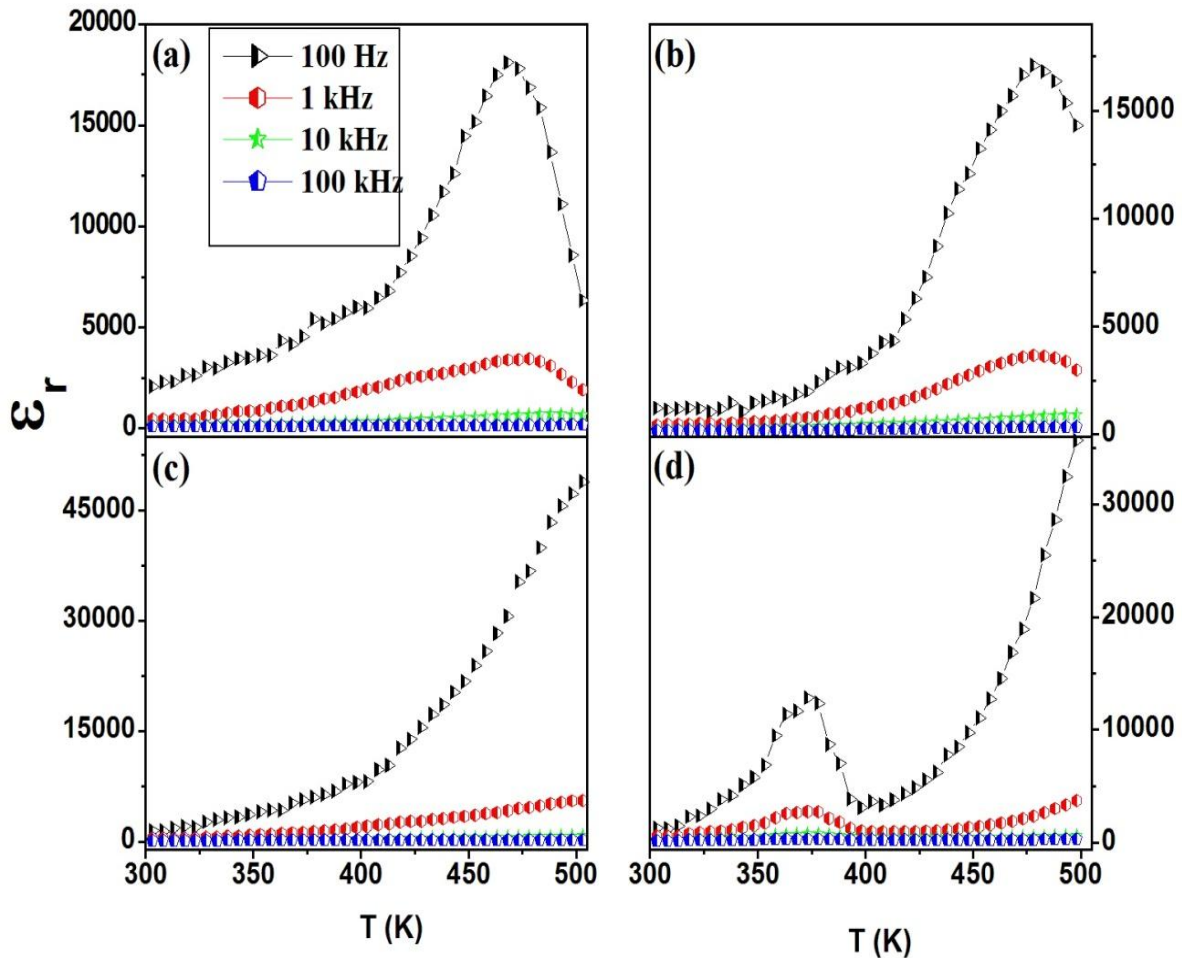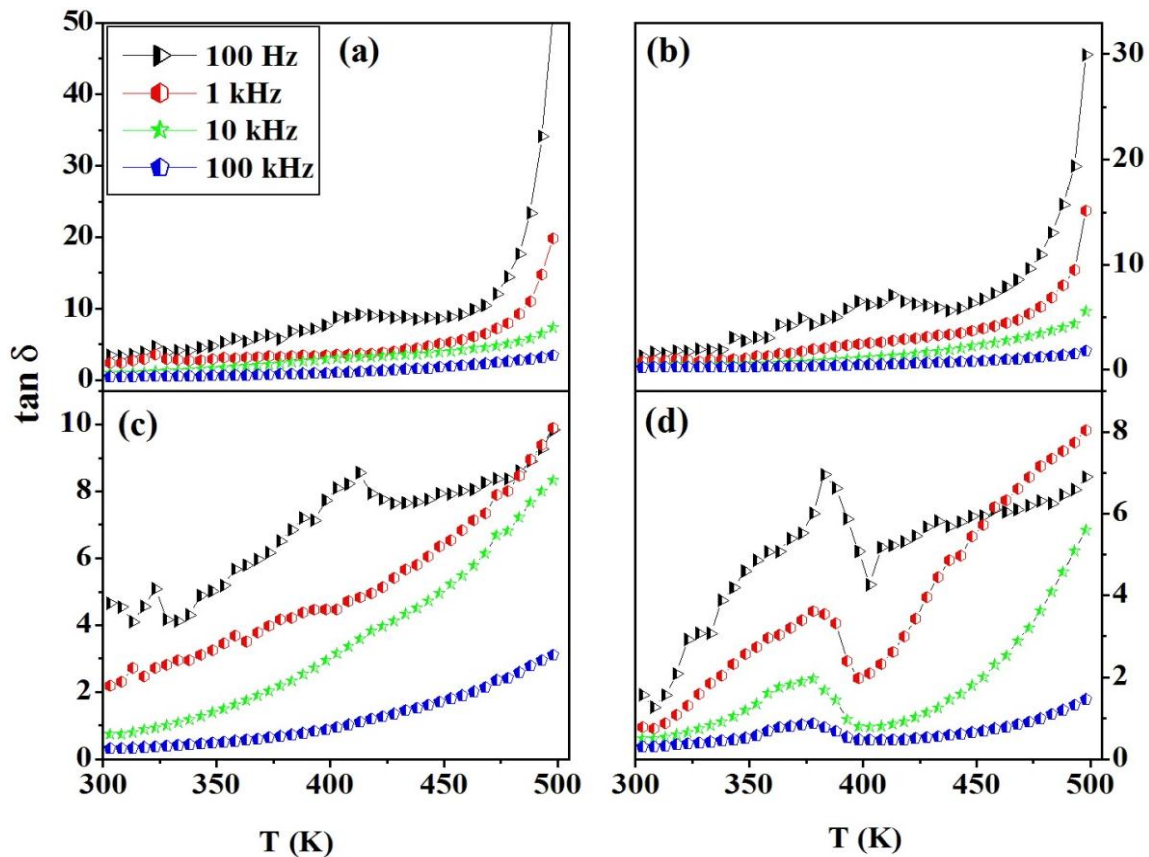

Figure 5.5. Plots of the dielectric constant (ε_r) versus temperature (T) of BT-BCT 5 nanocomposite sintered at 870 °C for (a) 4 h (b) 8 h (c) 12 h and (d) 16 h.

It clearly illustrates the presence of dielectric peaks with a variation of temperature. The peaks shifted to higher temperature regions with increasing sintering duration. The peak is more intense at 100 Hz, and the peak intensity decreases with

increasing frequency. The composite sintered at 870 °C for 16 h (Figure 5.5d) shows new peaks at 375 K besides high-temperature peaks. The presence of peaks around 450 °C in the composite may be due to dielectric relaxation. The dielectric constant of the BT-BCT 5 composite sintered for 12 h was found highest ($\varepsilon_r \approx$ 45000) at 100 Hz. The high dielectric constant of the composite is due to space charge polarization and chemical heterogeneities at the interface [Singh *et al*. (2014), Singh *et al*. (2015)].
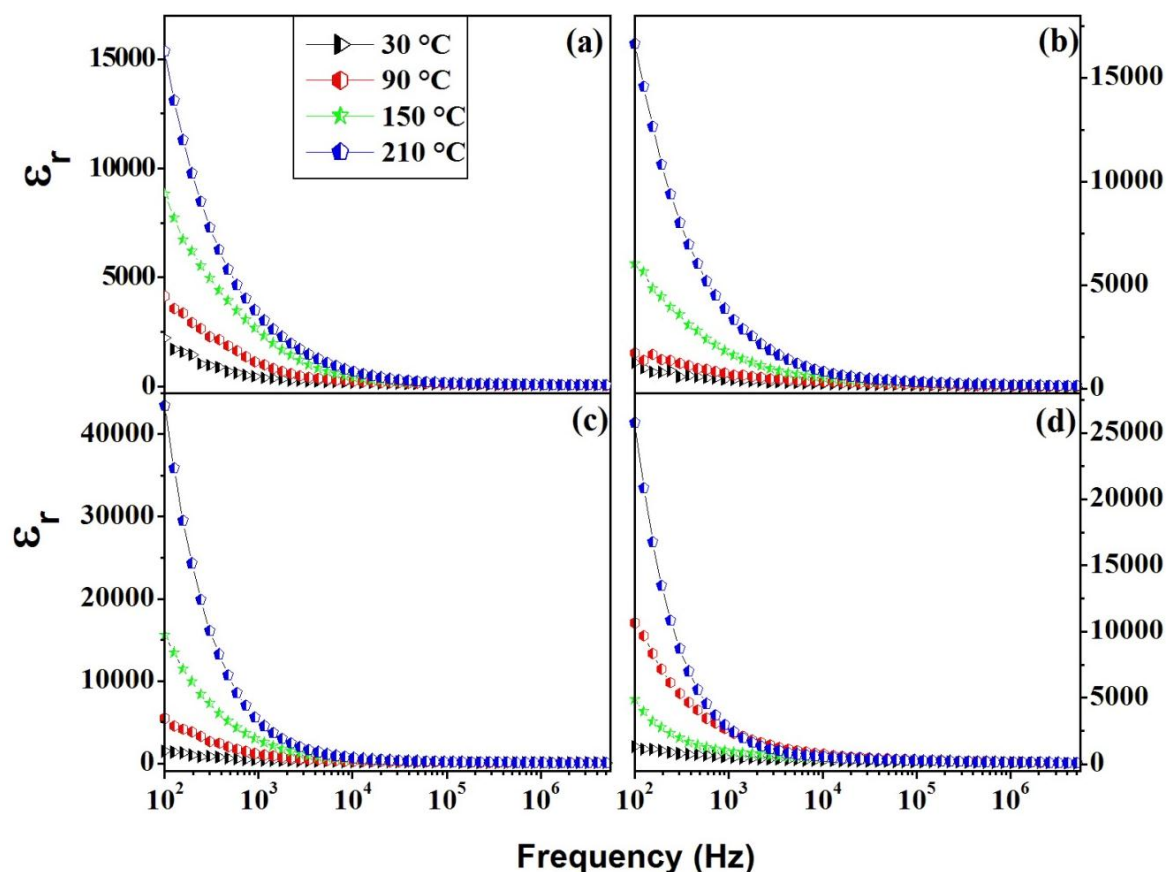
Figure 5.6 shows the plots of variation in dielectric loss (tan δ) with temperature for BT-BCT 5 composite at few selected frequencies (100 Hz, 1 kHz, 10 kHz, and 100 kHz). It is observed from the figures (a-d) that the dielectric loss gradually increases with sintering duration of 4 & 8 h whereas it increases sharply for the composite sintered for 12 and 16 h. Peaks are clearly resolved for the composite sintered for 16 h for all measured frequency (10^2 - 10^5 Hz) at 375 K. The value of dielectric loss for the composite sintered at 4, 8, 12 and 16 h at 100 kHz were found to be 0.39, 0.35, 0.22 and 0.24 respectively at 300 K. The dielectric loss peaks observed in the composite is due to thermally activated relaxation [Singh *et al*. (2014), Yadava *et al*. 2016].

Figure 5.6. Plots of dielectric loss (tan δ) versus Temperature (T) of BT-BCT 5 nanocomposite sintered   at 870 °C for (a) 4 h (b) 8 h (c) 12 h and (d) 16 h.

Figure 5.7 shows the plots of variation in dielectric constant (ε_r) as a function of frequency from 10^2 to 10^6 Hz at few selected temperatures for BT-BCT 5 nanocomposite. It is observed that the dielectric constant decreases rapidly below 1 kHz and then remains nearly constant between 10^4 to 10^6 Hz. The dielectric constant of the composite sintered at 870 °C for 12 h was found to be 43459 at 100 Hz and 483 K. The dielectric constant value decreases with increasing frequency while the dielectric constant increases at a given frequency with increasing temperature. The increase in ε_r with decreasing

frequency can be attributed to the contribution of charge accumulation at the interface. This leads to a Polarization is built up at insulating grain boundaries between the semiconducting grains of the ceramic samples which contributes to ε_r, whereas at high frequencies the periodic reversal of the field takes place so rapidly that there is no charge accumulation at the interface resulting in low dielectric constant (ε_r) value [Singh *et al.* (2013)].

Figure 5.7. Plots of dielectric constant (ε_r) versus Frequency of BT-BCT 5 nanocomposite sintered at 870 °C for (a) 4 h (b) 8 h (c) 12 h and (d) 16 h.

Figure 5.8 shows the variation in the dielectric loss (tan δ) with frequency (10^2 to 10^6 Hz) for the BT-BTC 5 nanocomposite sintered at 870 °C for 4, 8, 12 and 16 h and few selected temperatures. The tan δ versus frequency curve exhibits a distinct relaxation peaks which shift towards higher frequency side with increasing temperature. This behaviour may be explained by Maxwell-Wagner relaxation which is present in the BT-BCT 5 composite [Kumar *et al*. (2010)].
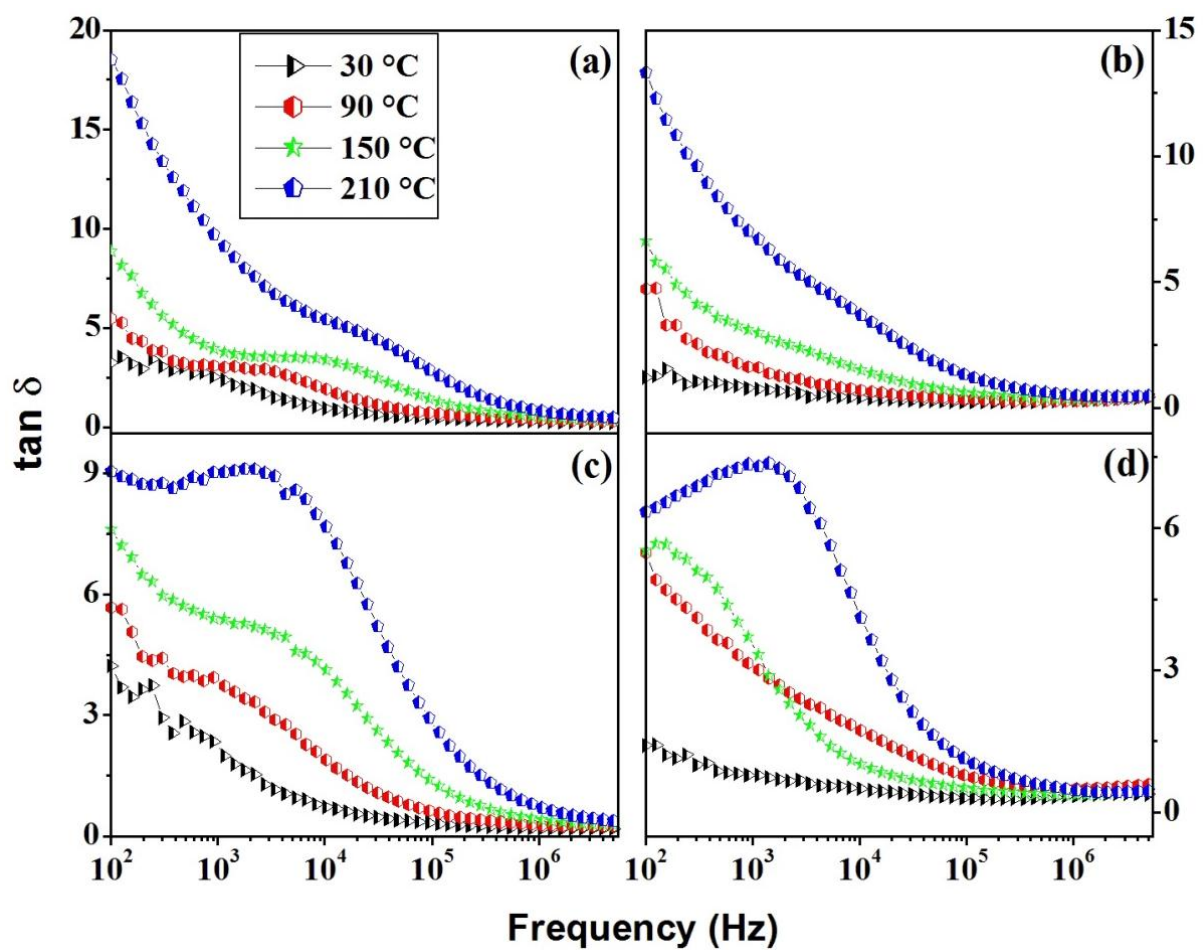
Figure 5.8. Plots of dielectric loss (tan δ) versus Frequency of BT-BCT 5 nanocomposite sintered at 870 °C for (a) 4 h (b) 8 h (c) 12 h and (d) 16 h.

5.4. Conclusion

A new nanocomposite of $0.5BaTiO_3$ - $0.5Bi_{2/3}Cu_3Ti_4O_{12}$ (BT-BCT 5) has been successfully synthesized for the first time by Solid state route. BCTO primary phase formation was confirmed by XRD at a lower temperature ($\leq$ 870 °C) compared to the conventional ceramic method. The particles size of the nanocomposite was in the range of 90 $\pm$ 10 nm. The average and RMS roughness of BT-BCT 5 composite were found to be 4.3 nm and 13.0 nm respectively with the help Atomic Force Microscope (AFM). The sample sintered at 870 °C for 12 h exhibited very high dielectric constant (ε_r) $\approx$ 48904 at 100 Hz and 503 K, and its loss tangent (tan δ) $\approx$ 0.32 at 100 kHz and 308 K. These results show that the nanocomposite has better dielectric properties than BCTO. The BT-BCT 5 nanocomposite shows temperature independent dielectric behaviour at higher frequencies but temperature dependent behaviour at low frequencies.